

# The Spin Stiffness and the Transverse Susceptibility of the Half-filled Hubbard Model

Zhu-Pei Shi and Rajiv R. P. Singh

*Department of Physics, University of California, Davis, California 95616*

## Abstract

The  $T = 0$  spin stiffness  $\rho_s$  and the transverse susceptibility  $\chi_\perp$  of the square lattice half-filled Hubbard model are calculated as a function of the Hubbard parameter ratio  $U/t$  by series expansions around the Ising limit. We find that the calculated spin-stiffness, transverse susceptibility, and sublattice magnetization for the Hubbard model smoothly approach the Heisenberg values for large  $U/t$ . The results are compared for different  $U/t$  with RPA and other numerical studies. The uniform susceptibility data indicate a crossover around  $U/t \approx 4$  between weak coupling (spin density wave) behavior at small  $U$  and strong coupling (Heisenberg) behavior at large  $U$ .

PACS numbers: 71.27.+a, 75.10.Jm, 75.40.Cx

Recent discovery of high- $T_c$  superconductivity in the Cuprate materials has generated tremendous interest in the subject of strongly correlated electrons. In these systems, the phenomena of unusual metallic behavior, antiferromagnetism and superconductivity occur in a narrow parameter range. It is widely believed that these phenomena have a common microscopic origin. The Hubbard model is one of the simplest models to describe correlated electron behavior in a solid. It consists of a single band of electrons, with nearest neighbor hopping parameter  $t$  and an on-site Coulomb repulsion between opposite spin electrons of magnitude  $U$ . The model is best understood at half-filling, that is, when there is one electron per unit cell, where the system becomes an antiferromagnetic insulator. At large values of  $U$  this system is well described by the Heisenberg model. At small  $U$  one expects the spin-density-wave (SDW) mean field description to become accurate. The possibility of  $d$ -wave superconductivity, away from half-filling, has been widely explored [1].

Direct calculations of the superconducting transition temperatures in the Hubbard model are beyond present numerical capabilities. Thus, phenomenological approaches, where the Hubbard model is used to determine the parameters in a scaling theory of superconductivity, are appropriate. If spin-fluctuations are important to the mechanism of superconductivity in the Cuprates, and if the magnetic excitations in the doped Cuprates are related to those in the stoichiometric insulating phases, the magnetic excitations in the half-filled system are clearly important for understanding superconductivity in these materials.

The magnetic ground state of the two-dimensional (2D) square lattice Hubbard model has been investigated by quantum Monte Carlo simulations [2–4] and Lanczos diagonalization [5]. These studies have mainly consisted of a finite size scaling analysis of the ground state properties of the model. They confirm the existence of long-range antiferromagnetic order at  $T = 0$ . To our knowledge, they have not been used to calculate the spin-stiffness constant or the spin-wave velocity for this model. Accurate numerical calculations of these quantities exist for the Heisenberg model. The Spin-density wave theory combined with the random phase approximation (RPA) has been used by Schrieffer et al. [6] to calculate the spin wave velocity for the Hubbard model. This calculation should become exact as  $U \rightarrow 0$ . Somewhat

surprisingly, it was found that the result of this calculation is also accurate in the Heisenberg limit ( $U/t \gg 1$ ).

In this Letter we *first* derive an expression for the spin stiffness constant of the Hubbard model by applying a slow twist in the ordering direction. We *then* introduce a one-parameter family of Hamiltonians which interpolate between the half-filled Hubbard and Ising models. This allows us to develop series expansions for the spin-stiffness. In addition, we develop series expansions for several thermodynamic parameters of this model, such as the uniform susceptibility and the sublattice magnetization. The spin wave velocity is calculated from the hydrodynamic relation [7]  $v_s^2 = \rho_s/\chi_\perp$ .

At large  $U$  our results extrapolate smoothly to the Heisenberg values. They also show good agreement with the spin-density wave theory at small  $U$ . The variation of the magnetic susceptibility with the Hubbard parameter ratio  $U/t$  shows a relatively well defined crossover between a  $\chi_\perp \sim U$  behavior at large  $U$  and  $\chi_\perp$  decreasing with increase in  $U$  at small  $U$ . This crossover between the strong coupling (Heisenberg model behavior) and weak coupling SDW behavior occurs at  $U/t \approx 4$ .

The Hubbard model is defined by the lattice Hamiltonian

$$H_0 = -t \sum_{\langle i,j \rangle, \sigma} (c_{i\sigma}^+ c_{j\sigma} + c_{j\sigma}^+ c_{i\sigma}) + U \sum_i (n_{i\uparrow} - \frac{1}{2})(n_{i\downarrow} - \frac{1}{2}) - \mu \sum_i (n_{i\uparrow} + n_{i\downarrow}) \quad , \quad (1)$$

where  $c_{i\sigma}^+$  and  $c_{i\sigma}$  are the creation and annihilation operators for electrons with a  $z$ -component of spin  $\sigma$  at lattice site  $i$ , and  $n_{i,\sigma} = c_{i\sigma}^+ c_{i\sigma}$ .  $U$  is the on site repulsive interaction,  $\mu$  the chemical potential, and  $t$  the nearest-neighbor hopping amplitude.

If we rotate the ordering direction by an angle  $\theta$  along a given direction such as  $y$  axis, then the spin stiffness constant  $\rho_s$  can be defined through the increase of the ground state energy:  $E_g(\theta) = E_g(\theta = 0) + \frac{1}{2} \rho_s \theta^2 + O(\theta^4)$ . This rotation can be carried out by the following transformation applied to the fermion operators:

$$\begin{pmatrix} c'_\uparrow \\ c'_\downarrow \end{pmatrix} = \begin{pmatrix} \cos \phi & \sin \phi \\ -\sin \phi & \cos \phi \end{pmatrix} \begin{pmatrix} c_\uparrow \\ c_\downarrow \end{pmatrix} \quad . \quad (2)$$

After rotation by a *relative* angle  $\theta$  ( that is letting  $\phi$  change by  $\theta/2$  ) between neighboring sites separated along  $y$  axis ( $\hat{y}$  denotes unit distance in  $y$  direction),  $H_0$  in Eq.(1) becomes  $H = H_0 + H^{dia} + H^{para} + O(\theta^3)$ , where

$$H^{dia} = \frac{t\theta^2}{8} \sum_{i,\sigma} (c_{i\sigma}^+ c_{i+\hat{y}\sigma} + c_{i+\hat{y}\sigma}^+ c_{i\sigma})$$

$$H^{para} = -\frac{t\theta}{2} \sum_i (c_{i\uparrow}^+ c_{i+\hat{y}\downarrow} - c_{i\downarrow}^+ c_{i+\hat{y}\uparrow} + c_{i+\hat{y}\downarrow}^+ c_{i\uparrow} - c_{i+\hat{y}\uparrow}^+ c_{i\downarrow}) .$$

The ‘‘diamagnetic’’ term  $H^{dia}$  is already of order  $\theta^2$  so for the calculation of the energy to order  $\theta^2$ , it can be replaced by its expectation value in the ground state of the  $\theta = 0$  Hamiltonian. We get  $\rho_s^{dia} = -\frac{1}{8} (Kinetic Energy) = -\frac{1}{8} [E_g(\theta = 0) - \frac{U}{2} (n - L)]$ , where  $n$  is a band filling, and  $L$  the local moment defined as  $L = \langle (n_{i\uparrow} - n_{i\downarrow})^2 \rangle$ . The contribution of the ‘‘paramagnetic’’ term  $H^{para}$  to the ground state energy in order  $\theta^2$  can be obtained from the expression,  $\rho_s^{para} = 2 \frac{\partial^2 E}{\partial \theta^2} |_{\theta=0}$ , where  $E$  is the energy of the Hamiltonian  $H_0 + H^{para}$ .

In order to calculate these quantities numerically, we introduce an Ising anisotropy into the Hubbard Hamiltonian:

$$H_{0\lambda} = -\lambda t \sum_{\langle i,j \rangle, \sigma} (c_{i\sigma}^+ c_{j\sigma} + c_{j\sigma}^+ c_{i\sigma}) + U \sum_i (n_{i\uparrow} - \frac{1}{2})(n_{i\downarrow} - \frac{1}{2}) + J(1 - \lambda) \sum_{\langle i,j \rangle} \sigma_i^z \sigma_j^z , \quad (3)$$

where  $\sigma_i^z = (n_{i\uparrow} - n_{i\downarrow})$  is the  $z$  component of the spin at site  $i$ , and  $J$  a parameter which can be tuned to improve the convergence of the extrapolations. The particle-hole symmetry ensures half-filling. For  $\lambda = 0$  the atomic limit of the Hubbard model is highly degenerate, however the Ising term selects from these the Néel states as the two degenerate ground states. Furthermore, this term also introduces a gap in the spectrum at  $\lambda = 0$ . *For  $\lambda = 1$  the Ising anisotropy goes to zero and the conventional Hubbard Hamiltonian is recovered.* Ground state properties of the model for  $\lambda \neq 0$  can be obtained by an expansion in powers of  $\lambda$ . If the gap does not close before  $\lambda = 1$  as expected for this model, we can obtain properties of the Hubbard model by extrapolating the expansions to  $\lambda = 1$ . In the strong coupling limit, the half-filled Hubbard model is equivalent to the Heisenberg model with

Hamiltonian  $-J_H \sum_{\langle i,j \rangle} (\sigma_i \cdot \sigma_j - 1)$  with  $J_H = t^2/U$ . The optimum value of the parameter  $J$  is found to be near  $J_H$  [8].

We calculate series coefficients for the ground state energy and the local moment to 11th order, and  $\rho^{para}$  to 9th order in  $\lambda$ . Using the Padé analysis, we obtain spin stiffness  $\rho_s = 0.186(15), 0.15(1), 0.077(7)$  and  $0.039(5)$  for  $U = 1, 4, 10$  and  $20$ , respectively. They are plotted in Fig. 1 as filled circles with errorbars. The dashed line is a guide to the eye. The errorbars represent the spread in the Padé estimates. At  $U = 20$ , our result ( $\rho_s U = 0.78$ ) can be compared to that (0.73) of the Heisenberg model [11]. Our results for  $\rho_s$  as well as  $M^\dagger$  are somewhat higher than the known results for the Heisenberg models. We believe this reflects the fact that the series have not converged as well as for the Heisenberg model and hence the reduction in these quantities due to the zero-point spin-wave fluctuations is not fully accounted for. Still, the convergence ( $\sim 5\%$ ) is quite reasonable.

We also compare our results with the Hartree-Fock approximation for the spin stiffness:  $\rho_s = -\frac{t}{2N} \sum_{\mathbf{k}} \frac{\epsilon(\mathbf{k}) \cos k_x}{E(\mathbf{k})}$ , where  $\epsilon(\mathbf{k}) = -2t(\cos k_x + \cos k_y)$  and  $E(\mathbf{k}) = [\epsilon^2(\mathbf{k}) + \Delta^2]^{1/2}$ .  $\Delta$  can be obtained by solving the gap equation  $\frac{U}{2N} \sum_{\mathbf{k}} \frac{1}{(\epsilon_{\mathbf{k}}^2 + \Delta^2)^{1/2}} = 1$ . The spin stiffness given by mean field solution of the gap equation is plotted in Fig. 1 as a solid line. One can see that this approximation overestimates the stiffness at large  $U$ . At  $U = 20$ , the mean field result is  $\rho_s U = 0.98$  compared to 0.73 for the Heisenberg model.

We note that the spin stiffness (filled squares in Fig. 1) from the variational Monte Carlo method with a Gutzwiller-type wave function are even larger than values of the mean field solution [9]. We believe that the large discrepancy is due to the missing spin flip processes in the Gutzwiller variational wave function used in [9]. Their calculations only get contributions to the spin-stiffness beyond the Hartree-Fock result from the ‘‘diamagnetic’’ term, whereas the ‘‘paramagnetic’’ part of the spin stiffness which contains spin-flip processes does not get corrected [10].

The transverse susceptibility of the Hubbard model can be defined in the usual way as  $4\chi_{\perp} = -2\frac{\partial^2 E}{\partial h^2} |_{h=0}$ , where  $E$  is the ground state energy of the Hamiltonian  $H_{0\lambda} - h \sum_i \sigma_i^x$ . The expansion coefficients of  $4\chi_{\perp}$  to 9th order in  $\lambda$  are also calculated.

The transverse susceptibility obtained from Padé approximants are  $4\chi_{\perp} = 0.94, 0.58, 0.75, 0.92$  and  $1.40$  for  $U = 1, 4, 6, 10$  and  $20$ , respectively. They are plotted in Fig. 2 as filled circles. A dashed line is a guide to the eye. At  $U = 20$ ,  $4\chi_{\perp}/U = 0.07$  is close to the large  $U$  limit value  $\chi_{\perp} J' = 0.065$  for the Heisenberg model [11] where  $J' = 4t^2/U$ . At  $U = 4$ , our result ( $4\chi_{\perp} = 0.58$ ) also agrees with the Monte Carlo Simulations ( $\approx 0.53$ ) by White *et al.* [3]. At  $U = 10$ , our result ( $4\chi_{\perp} = 0.92$ ) agrees with the Monte Carlo simulations of Moreo [4] (0.98). One can see in Fig. 2. that the variation of the magnetic susceptibility with  $U$  changes character around  $U = U_c \approx 4$ . It suggests that there is a crossover at  $U_c$  in the behavior of the 2D Hubbard model. For  $U > U_c$ , the magnetic susceptibility ( $4\chi_{\perp}$ ) is roughly proportional to  $U$  or inversely proportional to the spin superexchange  $J$ . This can be interpreted to imply that the magnetic state for  $U > U_c$  for 2D Hubbard model is close to the Heisenberg model. But, for  $U < U_c$ , the magnetic susceptibility ( $4\chi_{\perp}$ ) has qualitatively different behavior. It decreases as  $U$  increases. This can be interpreted as the weak coupling behavior of the SDW antiferromagnetic state.

We also compare our result with the mean field solutions of uniform magnetic susceptibility:  $\chi_{\perp} = \frac{1}{2U} [(1 - \Delta^2 U I_1 - U I_2^2/I_1)^{-1} - 1]$ , where  $I_1 = \frac{1}{2N} \sum_{\mathbf{k}} \frac{1}{E^3(\mathbf{k})}$  and  $I_2 = -\frac{1}{2N} \sum_{\mathbf{k}} \frac{\epsilon(\mathbf{k})}{E^3(\mathbf{k})}$ . It is plotted in Fig. 2 as a solid line. Again, we see that the mean field result is qualitatively correct, but overestimates the quantity especially at large  $U$ .

The spin wave velocity obtained from the relationship ( $\rho_s = v_s^2 \chi_{\perp}$ ) are  $v_s = 0.89, 1.02, 0.58$  and  $0.34$  for  $U = 1, 4, 10$  and  $20$ , respectively. They are plotted in Fig. 3 as filled circles with a solid line as a guide to the eye. At  $U = 20$ , our  $v_s = 0.34$  agrees well with the limiting value ( $v_s = 1.18\sqrt{2} J' = 0.33$ ) of the Heisenberg model [11].

We compare this result with the RPA solution of Schrieffer, Wen and Zhang [6]:  $v_s = [4t^2(1 - \Delta^2 U I_1) \frac{I_3}{I_1}]^{1/2}$ , where  $I_3 = \frac{1}{2N} \sum_{\mathbf{k}} \frac{\sin^2(k_x)}{E^3(\mathbf{k})}$ . It is plotted in Fig. 3 as a dotted line. We see that the RPA result for the spin wave velocity are lower than our series expansion results.

To summarize, in this paper we have derived an expression for the spin stiffness of the Hubbard model, and calculated it and other key long-wavelength parameters by systematic

series expansion methods. Comparison with the 2D  $S = 1/2$  Heisenberg antiferromagnet and RPA results, suggests that our extrapolations are good at small and large  $U$ . The uniform magnetic susceptibility data suggests a crossover between SDW behavior at small  $U$  and Heisenberg behavior at large  $U$  around  $U/t \approx 4$ .

This research was supported in part by NSF (DMR-9318537) and University Research Funds of the University of California at Davis. We would like to thank Prof. R. T. Scalettar and Prof. B. M. Klein for discussions.

## REFERENCES

- [1] See, for example, D. J. Scalapino, Phys. Rep. **250**, 329 (1995), and references therein.
- [2] J. E. Hirsch and S. Tang, Phys. Rev. Lett. **62**, 591 (1989).
- [3] S. R. White *et al.*, Phys. Rev. B **40**, 506 (1989).
- [4] A. Moreo, *et al.*, Phys. Rev. B **41**, 2313 (1990); A. Moreo, Phys. Rev. B **48**, 3380 (1993).
- [5] See, *e. g.* , E. Dagotto, A. Moreo and T. Barnes, Phys. Rev. B **40**, 6721 (1989).
- [6] J. R. Schrieffer, X. G. Wen and S. C. Zhang (SWZ), Phys. Rev. B **39**, 11663 (1989). A. Singh and Z. Tesanovic (ST) [Phys. Rev. B **41**, 614 (1990)] obtained a slightly different formula for the spin wave velocity from SWZ. We found that both formulae give almost the same results for  $U/t > 3$ , but for  $U/t < 3$  the ST formula decreases more slowly than that of SWZ as  $U/t$  decreases.
- [7] B. I. Halperin and P. C. Hohenberg, Phys. Rev. **188**, 898 (1969).
- [8] Zhu-Pei Shi and Rajiv R. P. Singh, to be published in Phys. Rev. B.
- [9] P. J. H. Denteneer and J. M. J. van Leeuwen, Europhysics Lett. **20**, 413 (1993).
- [10] The expectation value of the operator  $H^{para}$  between the Hartree-Fock and Gutzwiller wave functions is zero [P. J. H. Denteneer, G. An and J. M. J. van Leeuwen, Phys. Rev. B **47**, 6256 (1993)]. This suggests that one might improve the variational Monte Carlo method by adding a spin flip operator  $O_{sp}$  into the Gutzwiller-type wave function:

$$| \Psi_{GW} \rangle = \prod_i [1 - (1 - g)n_{i\uparrow} n_{i\downarrow} + p \times O_{sp}] | \Psi_{HF} \rangle$$

where  $p$  is a parameter and  $O_{sp} = (c_{i\uparrow}^+ c_{i+\hat{y}\downarrow} - c_{i\downarrow}^+ c_{i+\hat{y}\uparrow} + c_{i+\hat{y}\downarrow}^+ c_{i\uparrow} - c_{i+\hat{y}\uparrow}^+ c_{i\downarrow})$  .

- [11] R. R. P. Singh, Phys. Rev. B **39**, 9760 (1989); R. R. P. Singh and D. A. Huse, Phys. Rev. B **40**, 7247 (1989); C. J. Hamer *et al.*, Phys. Rev. B **50**, 6877 (1994).



## Figure Captions

Fig. 1 The spin stiffness as a function of  $U$ . Filled circles are our calculated data, with a dashed line as a guide to the eye. The errorbars indicate spread of the Padé approximants. The solid line is the mean field result. The filled squares are results of variational Monte Carlo simulations [9].

Fig. 2 Transverse susceptibility as a function of  $U$ . Filled circles are our calculated data, with a dashed line as a guide to the eye. A crossover between SDW and Heisenberg antiferromagnet is suggested around  $U \approx 4$ .

Fig. 3 The spin wave velocity as a function of  $U$ . Filled circles are our calculated data, with a solid line as a guide to the eye. The dotted line and dashed line represent results of RPA and Heisenberg antiferromagnet respectively.

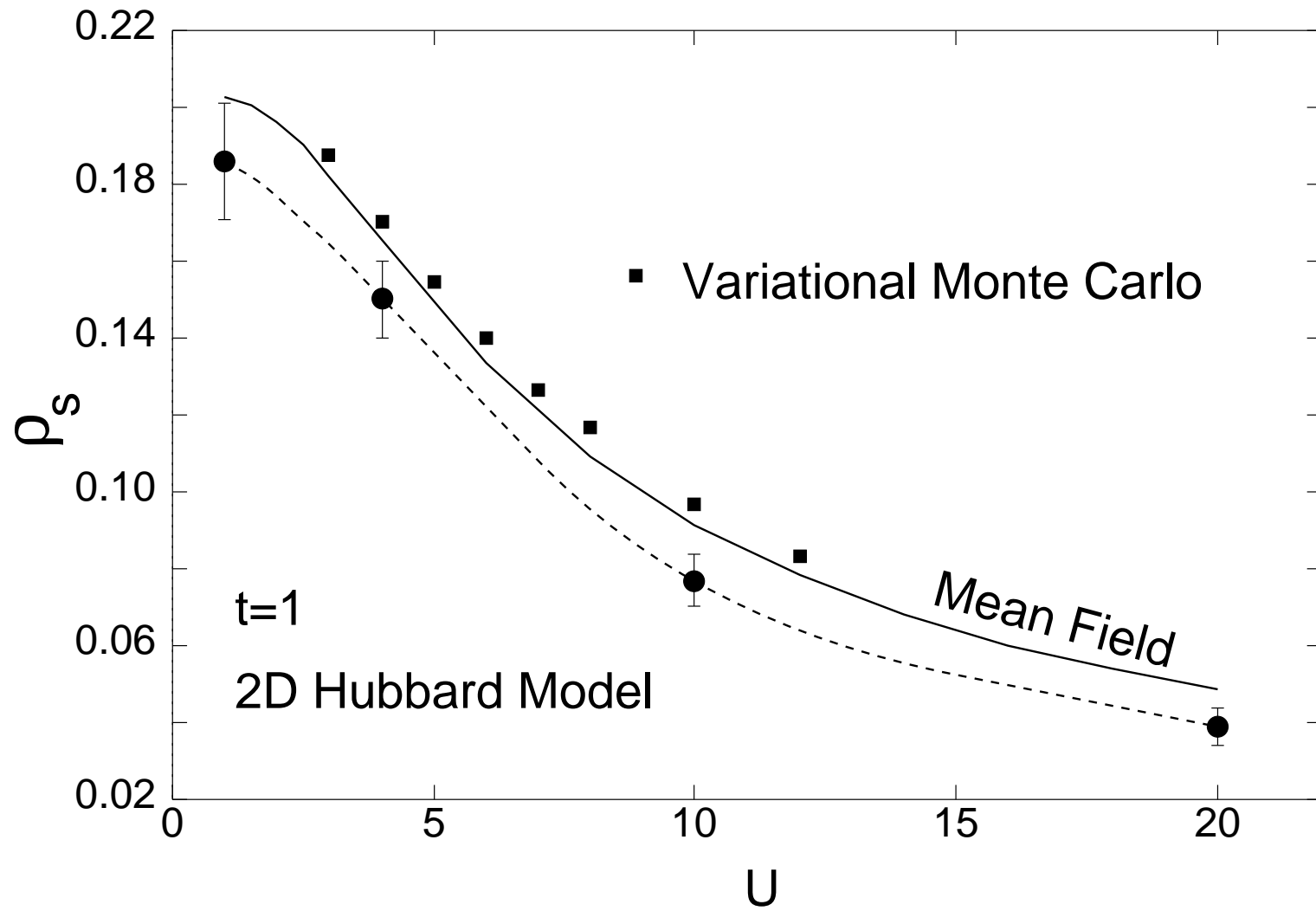


Fig. 1

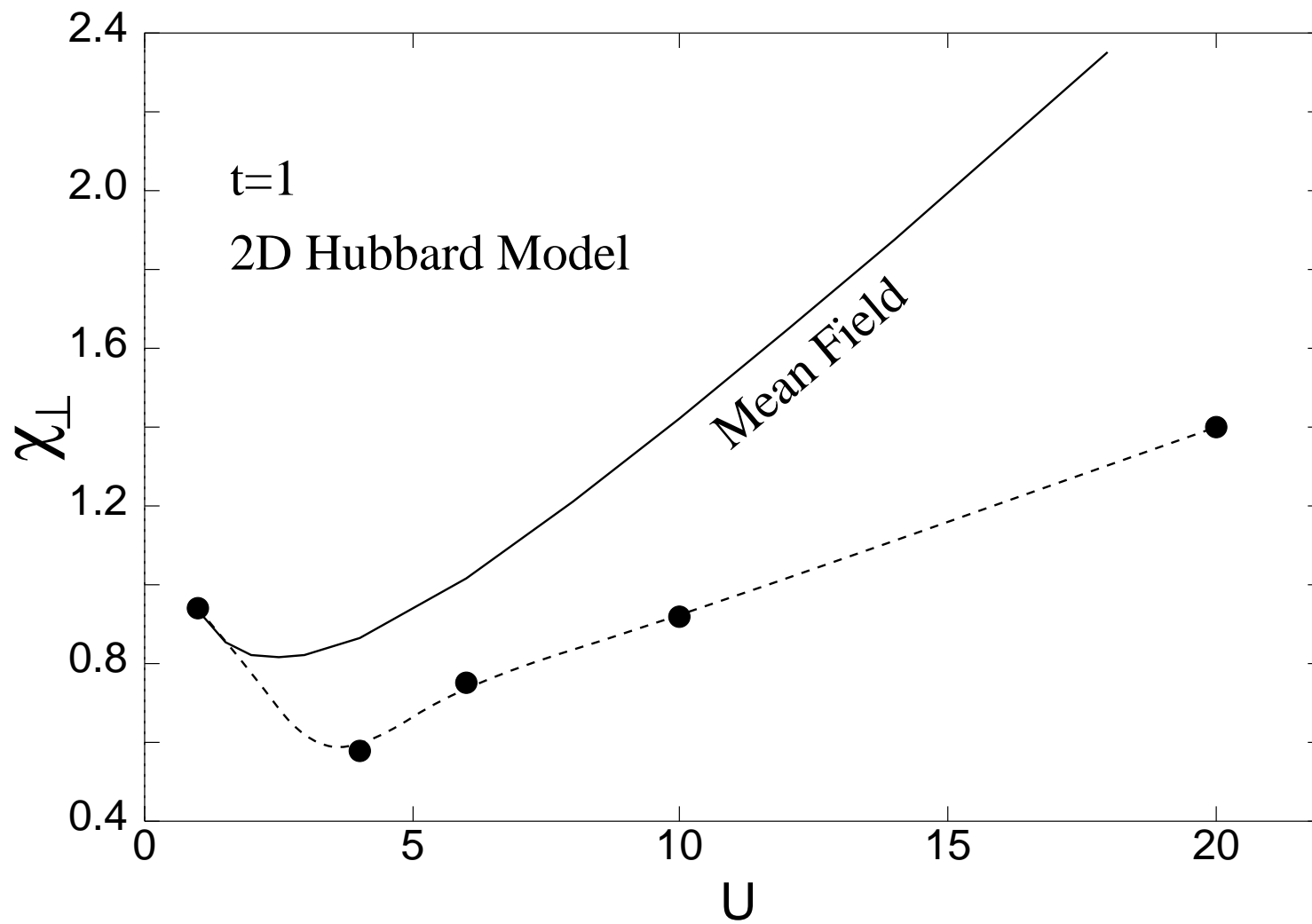


Fig. 2

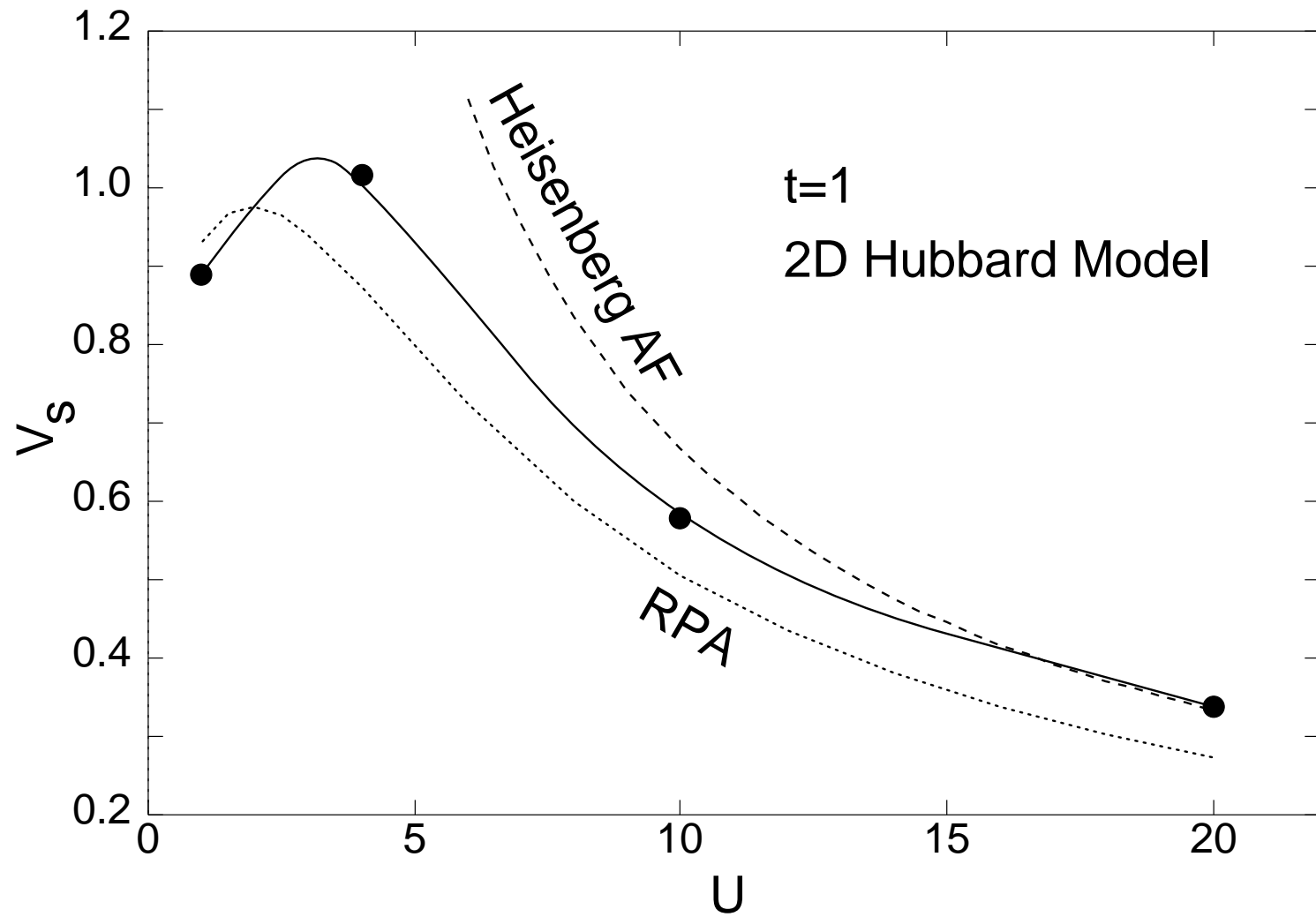


Fig. 3